J|A|C|S
ARTICLES

Published on Web 09/17/2010

High-Efficiency Green Organic Light-Emitting Devices Utilizing Phosphorescent Bis-cyclometalated Alkynylgold(III) Complexes

Vonika Ka-Man Au, Keith Man-Chung Wong, Daniel Ping-Kuen Tsang, Mei-Yee Chan,* Nianyong Zhu, and Vivian Wing-Wah Yam*

Institute of Molecular Functional Materials and Department of Chemistry, The University of Hong Kong, Pokfulam Road, Hong Kong

Received July 24, 2010; E-mail: wwyam@hku.hk

Abstract: A new phosphorescent material of cyclometalated alkynylgold(III) complex, [Au(2,5-$F_2C_6H_3$−C∧N∧C)(C≡C−$C_6H_4N(C_6H_5)_2$-*p*)] (**1**) (2,5-$F_2C_6H_3$−HC∧N∧CH = 2,6-diphenyl-4-(2,5-difluorophenyl)pyridine), has been synthesized, characterized, and its device performance investigated. This luminescent gold(III) complex was found to exhibit rich PL and EL properties and has been utilized as phosphorescent dopants of OLEDs. At an optimized dopant concentration of 4%, a device with a maximum external quantum efficiency (EQE) of 11.5%, corresponding to a current efficiency of 37.4 cd/A and a power efficiency of 26.2 lm/W, has been obtained. Such a high EQE is comparable to that of $Ir(ppy)_3$-based devices. The present work suggests that the alkynylgold(III) complex is a promising phosphorescent material in terms of both efficiency and thermal stability, with the additional advantages of its relatively inexpensive cost and low toxicity.

Introduction

Phosphorescent organic light-emitting diodes (OLEDs) or PHOLEDs have attracted considerable interest in recent years owing to their huge potential in full-color displays and solid-state lighting applications. One simple and effective approach toward the design of efficient phosphorescent materials would be to introduce heavy metal centers, such as iridium(III), platinum(II), ruthenium(II), and osmium(II), into organic molecules to facilitate the intersystem crossing from the singlet to the triplet states in order to harvest both the singlet and the triplet excitons, leading to 100% internal quantum efficiency. Extensive studies have been carried out on the design and synthesis of novel phosphorescent materials; particularly, much research work has been directed to the iridium(III) and platinum(II) systems[1−6] due to their ease of energy tuning via synthetic modification. As one of the primary colors, green OLEDs and PHOLEDs have attracted much attention, and *fac*-tris(2-phenylpyridine)iridium [$Ir(ppy)_3$] is one of the most widely employed green phosphorescent emitters for both monochromatic[7,8] and white OLEDs[9−11] by using the red-green-blue (RGB) approach. Owing to the extremely high photoluminescence (PL) quantum yield of nearly 100%,[12] the $Ir(ppy)_3$-doped device was reported to exhibit a peak external quantum efficiency (EQE) of 8.0% (28 cd/A) and power efficiency of 19 lm/W.[13] By employing a modified device structure with starburst perfluorinated phenylene compounds as hole- and exciton-blocking layer, the EQE of the $Ir(ppy)_3$-doped device can be further increased to 19.2%.[14] On the other hand, the development of phosphorescent emitters with metal centers other than the most commonly employed iridium(III) and platinum(II) for OLED applications has been relatively less explored. Thus the search for new classes of phosphorescent emitters with metal centers that are less expensive and of low toxicity and an environmentally benigned nature would be attractive. One candidate is the gold metal center, which is well-known for its inertness and low toxicity, as exemplified by its wide use in consumer goods, jewelry, and industry. The lack of gold compounds as triplet emitters for OLED applications stems from the lack of phosphorescent gold complexes that are thermally stable. While there have been a number of gold(I) compounds that are strongly phosphorescent,

(1) Adachi, C.; Baldo, M. A.; Forrest, S. R.; Lamansky, S.; Thompson, M. E.; Kwong, R. C. *Appl. Phys. Lett.* **2001**, *78*, 1622.
(2) Tokito, S.; Iijima, T.; Suzuri, Y.; Kita, H.; Tsuzuki, T.; Sato, F. *Appl. Phys. Lett.* **2003**, *83*, 569.
(3) Cocchi, M.; Fattori, V.; Virgili, D.; Sabatini, C.; Di Marco, P.; Maestri, M.; Kalinowshi, J. *Appl. Phys. Lett.* **2004**, *84*, 1052.
(4) Yan, B. P.; Cheung, C. C. C.; Kui, S. C. F.; Roy, V. A. L.; Che, C. M.; Xu, S. J. *Appl. Phys. Lett.* **2007**, *91*, 063508.
(5) Zhou, G.; Ho, C. L.; Wong, W. Y.; Wang, Q.; Ma, D.; Wang, L.; Lin, Z.; Marder, T. B.; Beeby, A. *Adv. Funct. Mater.* **2008**, *18*, 499.
(6) Gao, Z. Q.; Mi, B. X.; Tam, H. L.; Cheah, K. W.; Chen, C. H.; Wong, M. S.; Lee, S. T.; Lee, C. S. *Adv. Mater.* **2008**, *20*, 774.
(7) Adachi, C.; Baldo, M. A.; Forrest, S. R.; Thompson, M. E. *Appl. Phys. Lett.* **2000**, *77*, 904.
(8) He, G.; Pfeiffer, M.; Leo, K.; Hofmann, M.; Birnstock, J.; Pudzich, R.; Salbeck, J. *Appl. Phys. Lett.* **2004**, *85*, 3911.
(9) Sun, Y.; Giebink, N. C.; Kanno, H.; Ma, B.; Thomspon, M. E.; Forrest, S. R. *Nature* **2006**, *440*, 908.
(10) Schwartz, G.; Reineke, S.; Walzer, K.; Leo, K. *Appl. Phys. Lett.* **2008**, *92*, 053311.
(11) Reineke, S.; Linder, F.; Schwartz, G.; Seidler, N.; Walzer, K.; Lüssem, B.; Leo, K. *Nature* **2009**, *459*, 234.
(12) Kawamura, Y.; Goushi, K.; Brooks, J.; Brown, J. J.; Sasabe, H.; Adachi, C. *Appl. Phys. Lett.* **2005**, *86*, 071104.
(13) Baldo, M. A.; Lamansky, S.; Burrows, P. E.; Thompson, M. E.; Forrest, S. R. *Appl. Phys. Lett.* **1999**, *75*, 4.
(14) Ikai, M.; Tokito, S.; Sakamoto, Y.; Suzuki, T.; Taga, Y. *Appl. Phys. Lett.* **2001**, *79*, 156.

Scheme 1. Synthetic Route of **1**

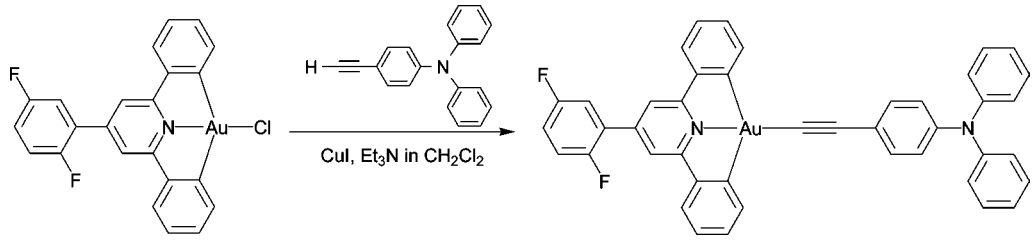

gold(III) compounds, on the other hand, are rarely luminescent at room temperature, which may be ascribed to the presence of non-emissive low-energy d-d ligand field states and the electrophilicity of the metal center.[15]

Recently, we reported the discovery of an entirely new class of luminescent neutral cyclometalated alkynylgold(III) complexes, [Au(C∧N∧C)(C≡C−R)], that exhibits strong PL in various media at both ambient and low temperatures.[15−17] The incorporation of strongly σ-donating alkynyl ligand into the gold(III) metal center has rendered the metal center more electron-rich and thus contribute to the enhancement of photophysical properties of the gold(III) complexes. More importantly, their photophysical properties and emission colors can be readily fine-tuned by modulating the ancillary ligands, significantly opening up the possibilities for the tailored design of novel gold(III) complexes. Taking the advantages that these cyclometalated alkynylgold(III) complexes are neutral and thermally stable, highly efficient OLEDs with EQE of 5.5% have been achieved by vacuum deposition of such luminescent compounds.[17] In light of our interest in luminescent metal alkynyls and functional materials for OLED applications, we have further extended our work to the design and synthesis of cyclometalated gold(III) complexes containing the dianionic ligands derived from more conjugated aryl-substituted diphenylpyridines (HC∧N∧CH). Herein, we report the synthesis, photophysical and electrochemical studies of an aryl-substituted cyclometalated alkynylgold(III) compound, [Au(2,5-$F_2C_6H_3$−C∧N∧C)(C≡C−$C_6H_4N(C_6H_5)_2$-*p*)] (**1**) (2,5-$F_2C_6H_3$−HC∧N∧CH = 2,6-diphenyl-4-(2,5-difluorophenyl)pyridine), and its application as a phosphorescent dopant in OLEDs. In particular, complex **1** has been found to exhibit rich electroluminescence (EL), yielding a highly efficient OLED with a peak EQE of 11.5%, corresponding to a current efficiency of 37.4 cd/A, and a power efficiency of 26.2 lm/W, comparable to those of the $Ir(ppy)_3$:CBP devices. In addition with the relatively lower cost and low toxicity of gold, such high EQE of the devices clearly demonstrated the attractiveness of this newly developed class of alkynylgold(III) complexes as superior candidates for the fabrication of phosphorescent OLEDs.

Results and Discussion

Synthesis and Characterizations. The tridentate ligand, 2,5-$F_2C_6H_3$−HC∧N∧CH,[18] and the precursor compound, [Au(2,5-$F_2C_6H_3$−C∧N∧C)Cl],[16] were prepared according to modified literature procedures, while complex **1** was synthesized *via* a copper-catalyzed route according to modification of a reported procedure (see Scheme 1).[15−17] The identity of **1** has been confirmed by ^{1}H NMR spectroscopy, FAB-mass spectrometry, IR spectroscopy, and satisfactory elemental analyses. The molecular structure has also been characterized by X-ray crystallography.

X-Ray Crystal Structure. Two independent molecules of **1** and one dichloromethane molecule were found in the asymmetric unit. In view of the identical molecular structure of the independent molecules with similar bond lengths and bond angles, only one of the molecule would be discussed in detail. The perspective view of one of the independent molecule of **1** (Figure 1a) shows a distorted square planar structure, in which the Au(III) metal center is coordinated to a tridentate 2,5-$F_2C_6H_3$−C∧N∧C ligand and a (4-diphenylamino-phenyl)ethynyl ligand, with C(1)−Au(1)−C(13) and N(1)−Au(1)−C(24) bond angles of 162.8(2) and 179.0(2)°, respectively. The bond lengths about the gold(III) center [Au(1)−C(1) 2.076(6), Au(1)−C(13) 2.067(6), Au(1)−N(1) 1.988(4), Au(1)−C(24) 1.966(5) Å] and the C(25)−C(24)−Au(1) bond angle of 174.4(6)° are normal and comparable to the related gold(III) complexes.[15,16] Crystal packing of **1** (Figure 1b) reveals the presence of partially stacked [Au(C∧N∧C)] units in a head-to-tail fashion and the shortest interplanar distance of 3.39 Å suggests the presence of aromatic π−π stacking interactions.

Photophysical Properties. Table 1 summarizes the photophysical properties of **1**. The UV−vis absorption spectrum of **1** in dichloromethane at room temperature shows a vibronic-structured low-energy absorption band at 390−410 nm (Figure 2), assignable to a metal-perturbed intraligand (IL) π−π* transition of the 2,5-$F_2C_6H_3$−C∧N∧C ligand, with some charge transfer character from the aryl ring to the pyridyl unit.[15−17,19,20] In addition to this vibronic-structured absorption band, an absorption tail that extends to 475−500 nm is also observed, which suggests the

(15) Yam, V. W.-W.; Wong, K. M.-C.; Hung, L.-L.; Zhu, N. *Angew. Chem., Int. Ed.* **2005**, *44*, 3107.
(16) Wong, K. M.-C.; Hung, L.-L.; Lam, W. H.; Zhu, N.; Yam, V. W.-W. *J. Am. Chem. Soc.* **2007**, *129*, 4350.
(17) Wong, K. M.-C.; Zhu, X.; Hung, L.-L.; Zhu, N.; Yam, V. W.-W.; Kwok, H. S. *Chem. Commun.* **2005**, 2906.
(18) Kröhnke, F. *Synthesis* **1976**, 1.
(19) Wong, K.-H.; Cheung, K.-K.; Chan, M. C.-W.; Che, C.-M. *Organometallics* **1998**, *17*, 3505.
(20) Au, V. K.-M.; Wong, K. M.-C.; Zhu, N.; Yam, V. W.-W. *J. Am. Chem. Soc.* **2009**, *131*, 9076.
(21) (a) Ichimura, K.; Kobayashi, T.; King, K. A.; Watts, R. J. *J. Phys. Chem.* **1987**, *91*, 6104. (b) Wang, X. Y.; Prabhu, R. N.; Schmehl, R. H.; Weck, M. *Macromolecules* **2006**, *39*, 3140. (c) Komamine, S.; Fujitsuka, M.; Ito, O. *Phys. Chem. Chem. Phys.* **1999**, *1*, 4745. (d) Guizzardi, B.; Mella, M.; Fagnoni, M.; Freccero, M.; Albini, A. *J. Org. Chem.* **2001**, *66*, 6353.
(22) (a) Tanaka, I.; Tabata, Y.; Tokito, S. *J. Appl. Phys.* **2006**, *99*, 073501. (b) Lee, J.; Chopra, N.; Eom, S.-H.; Zheng, Y.; Xue, J.; So, F.; Shi, J. *Appl. Phys. Lett.* **2008**, *93*, 123306.
(23) Goushi, K.; Kwong, R.; Brown, J. J.; Sasabe, H.; Adachi, C. *J. Appl. Phys.* **2004**, *95*, 7798.
(24) It is interesting to note that the EQE of the devices is considerably higher than that expected from the PL quantum yield measurements, which may be ascribed to the lack of efficient energy transfer pathway from the host to the phosphorescent dopant. This is consistent with the observation reported by Kawamura *et al.*, in which the PL quantum yields of organic thin films are strongly dependent on the use of host materials and the measurement environment, Kawamura, Y.; Goushi, K.; Brooks, J.; Brown, J. J.; Sasabe, H.; Adachi, C. *Appl. Phys. Lett.* **2005**, *86*, 071104.

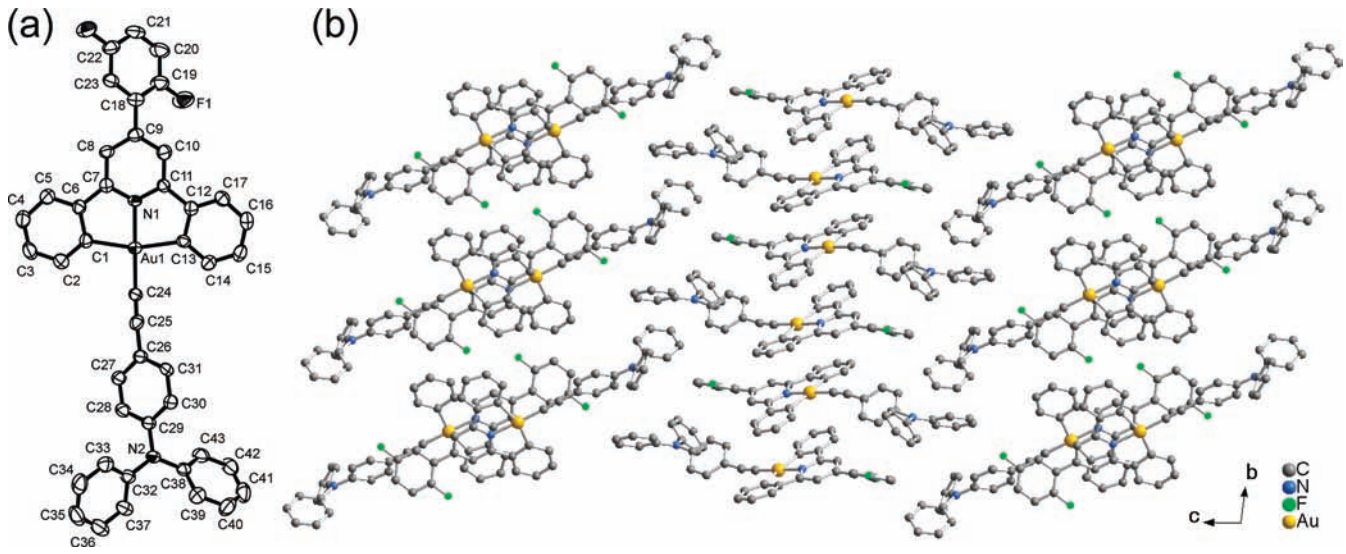

Figure 1. (a) Molecular structure of one of the independent molecules of **1** with atomic numbering scheme. Hydrogen atoms are omitted for clarity. Thermal ellipsoids are drawn at the 40% probability level. (b) Crystal packing of **1** viewed along *a* axis.

Table 1. **Photophysical Data for 1**

	absorption[a]	emission		
complex	λ_{max}/nm (ε_{max}/dm^3 mol^{-1}cm^{-1})	medium (*T*/K)	λ_{max}/nm (τ_0/μs)	Φ_{em}[b]
1	316 (45915), 392 (7835), 410 (825)	CH_2Cl_2 (298)	669 (<0.05)	8.5×10^{-3}
		solid (298)	590 (<0.05, 0.2)[e]	
		solid (77)	580 (1.5, 8.1)[e]	
		glass (77)[c,d]	478, 512, 532 (366)	
		thin film (298)		
		2% in PMMA	537	0.34
		4% in PMMA	538	
		8% in PMMA	543	
		20% in PMMA	558	
		50% in PMMA	577	

[a] In dichloromethane at 298 K. [b] The luminescence quantum yield, measured at room temperature using quinine sulfate as a standard. [c] Vibronic-structured emission band. [d] In EtOH−MeOH−CH_2Cl_2 (40:10:1 v/v). [e] Double exponential decay.

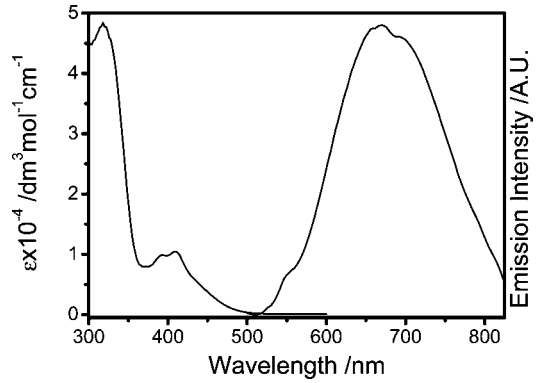

Figure 2. UV−vis absorption and emission spectra of compound **1** in dichloromethane at 298 K.

possibility of an admixture of an intraligand (IL) $\pi-\pi^*$ [2,5-$F_2C_6H_3$−C∧N∧C and C≡C−$C_6H_4N(C_6H_5)_2$-*p*] and a ligand-to-ligand charge transfer (LLCT) π[C≡C−$C_6H_4N(C_6H_5)_2$-*p*] → π^*(2,5-$F_2C_6H_3$−C∧N∧C) transition in the low-energy absorption bands due to the presence of the electron-rich $-N(C_6H_5)_2$ substituent on the alkynyl moiety. In dichloromethane solution (in the range $2.0 \times 10^{-5}-1.0 \times 10^{-3}$ mol dm^{-3}) at room temperature, **1** shows a broad structureless emission band at ~669 nm upon excitation at 470 nm (Figure 2). With reference to spectroscopic studies on the related compounds,[15−17] this low-energy structureless band is assigned as derived from an excited state of ^{3}LLCT [π(C≡C−$C_6H_4N(C_6H_5)_2$-*p*) → π^*(2,5-$F_2C_6H_3$−C∧N∧C)] origin due to the presence of the energetically higher-lying π(C≡C−$C_6H_4N(C_6H_5)_2$-*p*) orbital resulting from the strongly electron-donating $-N(C_6H_5)_2$ substituent on the alkynyl ligand. In the solid-state thin film, **1** displays a similar low-energy structureless emission band with emission energies showing a concentration dependence when doped in PMMA. The emission energies were found to shift from 538 to 575 nm in the concentration range of 2 to 50 wt % in PMMA and further to 588 nm in the solid state (Figure 3). The observation of such concentration-dependent emission energies is probably due to excimeric emission resulting from the π-stacking of the 2,5-$F_2C_6H_3$−C∧N∧C moieties with higher order and better packing of molecules at higher concentrations, as supported by the observation of such $\pi-\pi$ stacking in the crystal packing of **1** (Figure 1b).

(25) McIlroy, S. P.; Cló, E.; Nikolajsen, L.; Frederiksen, P. K.; Nielsen, C. B.; Mikkelsen, K. V.; Gothelf, K. V.; Ogilby, P. R. *J. Org. Chem.* **2005**, *70*, 1134.
(26) (a) Demas, J. N.; Crosby, G. A. *J. Phys. Chem.* **1971**, *75*, 991. (b) van Houten, J.; Watts, R. *J. Am. Chem. Soc.* **1976**, *98*, 4853.
(27) (a) Che, C. M.; Wong, K. Y.; Anson, F. C. *J. Electroanal. Chem., Interfacial Electrochem.* **1987**, *226*, 211. (b) Connelly, N. G.; Geiger, W. E. *Chem. Rev.* **1996**, *96*, 877.

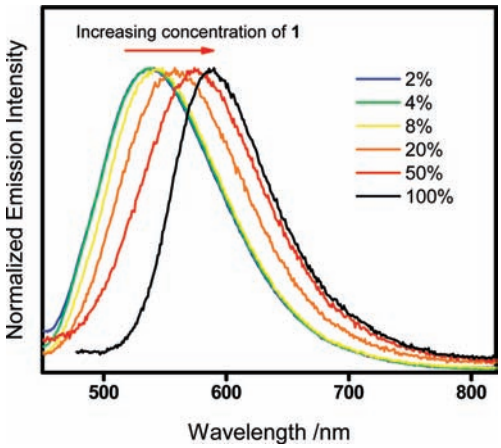

Figure 3. Normalized photoluminescence spectra of **1** at different concentrations (wt %) in PMMA thin films at 298 K.

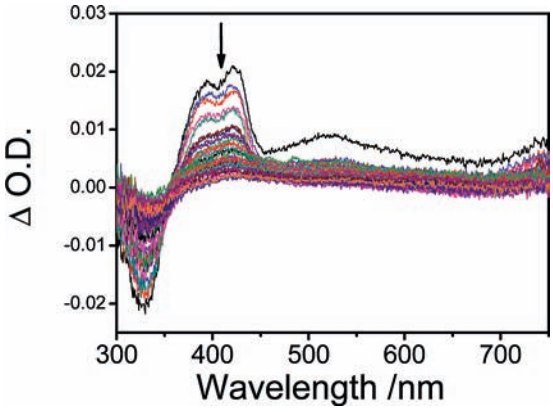

Figure 4. Transient absorption spectra of **1** in CH_2Cl_2 at room temperature at decay times of 0−300 μs.

Nanosecond UV−Vis Transient Absorption (TA) Spectroscopy. In order to obtain more information on the nature of the excited state, nanosecond transient absorption (TA) measurements were performed on complex **1** in degassed dichloromethane solution at room temperature. The TA-difference spectra of **1** determined at different delay times after a 355 nm laser pulse excitation are shown in Figure 4. The transient absorption difference spectrum is characterized by a ground-state bleaching at ∼300−350 nm and two intense positive absorption bands centered at ∼390−420 and 520 nm. The bleaching is ascribed to the depletion of ground-state lowest-energy absorption band, which is assigned as an intraligand $\pi-\pi^*$ transition of the C∧N∧C ligand. On the basis of a literature report on Ir(III) complexes containing ppy ligand,[21a,b] the higher-energy band at 390−420 nm is assigned as an absorption typical of triplet absorption of cyclometalated C∧N∧C derivatives. On the other hand, the absorption band at ∼520 nm is tentatively assigned as the (4-diphenylaminophenyl)ethynyl radical cation absorption. A similar TA band has also been observed for the radical cation of free 4-aminophenylacetylene[21c] and the related aniline and chloroaniline molecules.[21d] The observation of such characteristic radical cation absorption suggested the formation of the charge-separated state, which is in line with the assignment of the origin of excited state as derived from ^{3}LLCT [π(C≡C−$C_6H_4N(C_6H_5)_2$-*p*) → π^*(2,5-$F_2C_6H_3$−C∧N∧C)] transition. It is likely that the absorption due to the C∧N∧C radical anion is masked as it is expected to appear at ∼380−420 nm, close to the region where ground-state bleaching occurs.

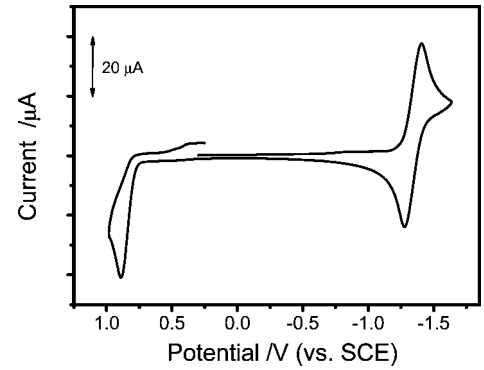

Figure 5. Cyclic voltammogram of **1** in CH_2Cl_2 (0.1 mol dm^{-3} $^nBu_4NPF_6$).

Electrochemistry. The cyclic voltammograms of **1** in dichloromethane (0.1 mol dm^{-3} $^nBu_4NPF_6$) showed one quasi-reversible reduction couple at −1.35 V and one irreversible oxidation wave at +0.89 V (vs SCE). The cyclic voltammogram of **1** is shown in Figure 5. On the basis of the related electrochemical studies on similar cyclometalated alkynylgold(III) complexes,[16] the reduction process is assigned as the 2,5-$F_2C_6H_3$−C∧N∧C ligand-centered reduction. The observation of a less negative potential for the reduction couple, relative to the other related analogues containing the unsubstituted C∧N∧C ligand, is attributed to the presence of the lower-lying π^* orbital associated with the difluorophenyl substituent on the 2,5-$F_2C_6H_3$−C∧N∧C ligand. The oxidation wave at +0.89 V is assigned as an alkynyl ligand-centered oxidation. Similar oxidation wave was also observed for other related cyclometalated alkynylgold(III) complexes containing the same −C≡C−$C_6H_4N(C_6H_5)_2$-*p* ligand.

Electroluminescence Properties. A knowledge of the electrochemical data, together with the photophysical results, have provided the information on the energies of the highest occupied molecular orbital (HOMO) and the lowest unoccupied molecular orbital (LUMO) as well as the triplet state energies of **1**, which are essential for the judicious choices of hole- and electron-transporting materials for the fabrication of OLEDs. In view of the fact that a relatively high luminescence quantum yield of 34% was found in a 2 wt % of **1** doped in PMMA, together with its high thermal stability as revealed by its high decomposition temperature of >460 °C in the thermogravimetric analysis, compound **1** is anticipated to exhibit a promising potential as a candidate of phosphorescent emitting material for the fabrication of high performance OLEDs.

Figure 6 shows the normalized EL spectra of the devices with different concentrations of **1** doped into the CBP layer viewed at the normal direction at a current density of 20 mA/cm^2. The EL spectra are peaked at ∼528 nm with full width at half maxima (fwhm) of 90 nm (3106 cm^{-1}) and CIE coordinates of (0.34, 0.57), resembling that of the PL spectrum in the solid thin film. As the concentration of **1** increases, the EL band maxima are found to be slightly red-shifted from 528 to 532 nm, which is consistent with the concentration dependence observed in the PL spectra. This confirms that a high dopant concentration of **1** would give rise to a higher molecular order and a better packing of the molecules, leading to a stronger π-stacking of the C∧N∧C ligand, and hence a lower energy dimeric/oligomeric or excimeric intraligand EL is observed.[17]

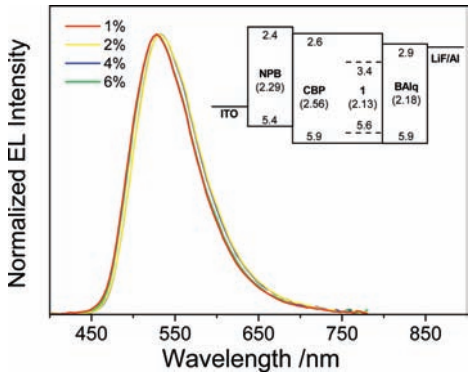

Figure 6. Normalized EL spectra of the devices with different concentrations of **1** doped into the CBP layer at a current density of 20 mA/cm^2. Inset: Proposed energy band diagram for the OLED. Note that numbers indicate the respective highest occupied and lowest unoccupied molecular orbital (HOMO and LUMO, respectively) energies relative to the vacuum as well as the triplet energy levels (in parentheses) in eV.

The observation of $\pi-\pi$ stacking in the crystal packing of **1** (*vide supra*) may account for the occurrence of the dimeric/oligomeric or excimeric emission. It is worth noting that the unwanted NPB emission is suppressed in the present devices, unlike in the case of previous studies with other cyclometalated alkynylgold(III) complexes.[17] Of particular interest is that only green emission from **1** can be observed, and the EL spectra do not consist of any other residual emission from either the host or the adjacent hole- or electron-transporting layer even at high current density, indicating complete energy transfer from the CBP host exciton to the triplet state of **1** upon electrical excitation. This improvement can be rationalized in terms of the effectiveness of the carrier confinement layer inserted between the the hole-transporting layer (HTL) and the emissive layer (EML). The inset of Figure 6 depicts the proposed energy band diagram of the OLED, in which the HOMO and the LUMO of the organic materials employed were extracted from the literature,[22] and those of **1** were estimated from the CV data (*vide supra*). Apparently, efficient energy transfer from the CBP to the triplet state of **1** is expected, as the triplet energies of complex **1** and CBP are 2.13 and 2.56 eV,[23] respectively. More importantly, the insertion of the thin CBP layer (~5 nm thick) can effectively confine the triplet excitons within the EML and can also suppress the unwanted energy transfer from the triplet excitons of **1** to the non-radiative NPB triplet states, owing to its triplet energy (2.56 eV) being higher than that of NPB (2.29 eV).[23]

Figure 7 depicts the current and power efficiencies and the EQE of the devices with different concentrations of **1** doped into the CBP layer as a function of current density. At an optimized dopant concentration of 4%, the device exhibits a maximum current efficiency of 37.4 cd/A and a maximum power efficiency of 26.2 lm/W. However, a gradual decrease of current efficiency and power efficiency is observed at high current density. For example, at a luminance of 100 cd/m^2, the current and power efficiencies drop to 22.0 cd/A and 9.0 lm/W, respectively. This efficiency roll-off may be attributed to the triplet−triplet annihilation that is commonly observed in the phosphorescent OLEDs. Apparently, the EQE of the devices increases with increasing concentration of **1**, and achieves a peak EQE of 11.5% for the optimized concentration of 4%. Such a high EQE is comparable to that of the optimized Ir(ppy)$_3$:CBP devices reported.[13,14,24] This suggests that alkynylgold(III)

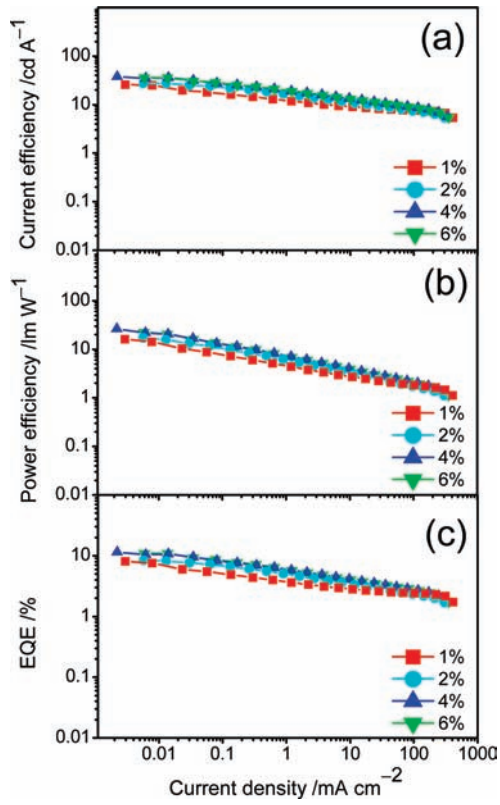

Figure 7. (a) Current and (b) power efficiencies and (c) external quantum efficiencies (EQE) of the devices with different concentrations of **1** doped into the CBP layer as a function of current density.

complex **1** is a superior candidate as phosphorescent dopant for OLEDs, in addition to its relatively lower cost and low toxicity.

Conclusion

We reported the synthesis, characterization, and device performance investigation of a new phosphorescent material, [Au(2,5-$F_2C_6H_3$−C∧N∧C)(C≡C−$C_6H_4N(C_6H_5)_2$-*p*)] (**1**) (2,5-$F_2C_6H_3$−HC∧N∧CH = 2,6-diphenyl-4-(2,5-difluorophenyl)pyridine). This luminescent cyclometalated alkynylgold(III) complex exhibits rich PL and EL properties and has been utilized as phosphorescent dopants of OLEDs. At an optimized dopant concentration of 4%, a device with a maximum EQE of 11.5%, corresponding to a current efficiency of 37.4 cd/A and a power efficiency of 26.2 lm/W has been obtained. Such a high EQE is comparable to that of Ir(ppy)$_3$-based devices. The present work suggests that the alkynylgold(III) complex is a promising phosphorescent material in terms of both efficiency and thermal stability, with the additional advantage of its relatively inexpensive cost and low toxicity.

Experimental Section

Materials and Reagents. Potassium tetrachloroaurate(III) was purchased from Strem. 2,5-$F_2C_6H_3$−HC∧N∧CH,[18] (4-diphenylamino-phenyl)ethyne,[25] and the precursor compound [Au(2,5-$F_2C_6H_3$−C∧N∧C)Cl][15−17] were prepared by modification of the literature procedures. All solvents were purified and distilled using standard procedures before use. All other reagents were of analytical grade and were used as received. Tetra-*n*-butylammonium hexafluorophosphate (Aldrich) was recrystallized twice from absolute ethanol before use.

Physical Measurements and Instrumentation. UV−Visible spectra were obtained on a Hewlett-Packard 8452A diode array

spectrophotometer, IR spectra as KBr disk on a Bio-Rad FTS-7 Fourier transform infrared spectrophotometer (4000−400 cm^{-1}). ^1H NMR spectra were recorded on a Bruker DPX-300 (300 MHz) Fourier transform NMR spectrometer with chemical shifts recorded relative to tetramethylsilane (Me_4Si). Positive-ion FAB mass spectra were recorded on a Finnigan MAT95 mass spectrometer. Elemental analyses for the metal complexes were performed on the Carlo Erba 1106 elemental analyzer at the Institute of Chemistry, Chinese Academy of Sciences, Beijing, China. Steady-state excitation and emission spectra were recorded on a Spex Fluorolog-2 model F 111 fluorescence spectrofluorometer equipped with a Hamamatsu R-928 photomultiplier tube. Solid-state photophysical measurements were carried out with the solid sample loaded in a quartz tube inside a quartz-walled Dewar flask. Liquid nitrogen was placed into the Dewar flask for low temperature (77 K) photophysical measurements. Excited-state lifetimes of solution samples were measured using a conventional laser system. The excitation source used was the 355-nm output (third harmonic, 8 ns) of a Spectra-Physics Quanta-Ray Q-switched GCR-150 pulsed Nd:YAG laser (10 Hz). Luminescence quantum yields for solution samples were measured by the optical dilute method reported by Demas and Crosby[26a] with a degassed aqueous solution of quinine sulfate ($\Phi = 0.546$, excitation wavelength at 365 nm) as the reference,[26b] while those of the thin films were measured on a Hamamatsu C9920-03 Absolute PL Quantum Yield Measurement System. Transient absorption measurements were performed on a LP920-KS Laser Flash Photolysis Spectrometer (Edinburgh Instruments Ltd., Livingston, UK) at ambient temperature. The excitation source was the 355 nm output (third harmonic) of a Nd:YAG laser (Spectra-Physics Quanta-Ray Lab-130 Pulsed Nd:YAG Laser), and the probe light source was a Xe900 450 W xenon arc lamp. The transient absorption spectra were detected by an image-intensified CCD camera (Andor) with PC plug-in controller, fully operated by L900 spectrometer software. The absorption kinetics were detected by a Hamamatsu R928 photomultiplier tube and recorded on a Tektronix model TDS3012B (100 MHz, 1.25 GS/s) digital oscilloscope and analyzed using the same software for exponential fit (tail-fit data analysis). All solution samples for photophysical studies were freshly prepared under a high vacuum in a 10-cm^3 round-bottomed flask equipped with a side-arm, 1-cm fluorescence cuvette and sealed from the atmosphere by a Rotaflo HP6/6 quick-release Teflon stopper. Solutions were rigorously degassed on a high-vacuum line in a two-compartment cell with no less than four successive freeze−pump−thaw cycles. Cyclic voltammetric measurements were performed by using a CH Instruments, Inc. model CHI 600A electrochemical analyzer. The electrolytic cell used was a conventional two-compartment cell. Electrochemical measurements were performed in dichloromethane solutions with 0.1 M $^nBu_4NPF_6$ as supporting electrolyte at room temperature. The reference electrode was a $Ag/AgNO_3$ (0.1 M in acetonitrile) electrode, and the working electrode was a glassy carbon electrode (CH Instruments, Inc.) with a platinum wire as the counter electrode. The working electrode surface was first polished with 1 μm alumina slurry (Linde), followed by 0.3 μm alumina slurry, on a microcloth (Buehler Co.). Treatment of the electrode surfaces was as reported previously.[27a] The ferrocenium/ferrocene couple ($FeCp_2^{+/0}$) was used as the internal reference.[27b] All solutions for electrochemical studies were deaerated with pre-purified argon gas just before measurements.

Crystal Structure Determination. Single crystals of **1** suitable for X-ray diffraction studies were grown by layering *n*-hexane onto a concentrated dichloromethane solution of **1**. The X-ray diffraction data were collected on a Bruker Smart CCD 1000 using graphite monochromatized Mo−Kα radiation ($\lambda = 0.71073$ Å). Raw frame data were integrated with the SAINT[28] program. Semi-empirical absorption correction with SADABS[29] was applied. The structure was solved by direct methods employing the SHELXS-97 program.[30] Full-matrix least-squares refinement on F^2 was used in the structure refinement. The positions of H atoms were calculated on the basis of the riding mode with thermal parameters equal to 1.2 times that of the associated C atoms, and these positions participated in the calculation of final *R* indices. In the final stage of least-squares refinement, all non-hydrogen atoms were refined anisotropically.

Synthesis and Characterization of 1. Complex **1** was synthesized by reaction of [Au(2,5-$F_2C_6H_3$−C∧N∧C)Cl] with (4-diphenylamino-phenyl)ethyne in the presence of a catalytic amount of copper(I) iodide in triethylamine and dichloromethane. **1**: ^1H NMR (300 MHz, CD_2Cl_2, 298 K, relative to Me_4Si): δ 7.06 (m, 4H, C≡CC_6H_4 and N(C_6H_5)$_2$), 7.10 (d, $J = 8.7$ Hz, 4H, N(C_6H_5)$_2$), 7.24−7.30 (m, 8H, phenyl of N(C_6H_5)$_2$, 2,5-$F_2C_6H_3$ and C_6H_4 of C∧N∧C), 7.36−7.43 (m, 5H, C≡CC_6H_4 2,5-$F_2C_6H_3$ and C_6H_4 of C∧N∧C), 7.63 (m, 4H, pyridyl and C_6H_4 of C∧N∧C), 8.01 (d, $J = 6.1$ Hz, 2H, C_6H_4 of C∧N∧C); positive FAB-MS: *m/z* 808 $[M]^+$; IR (KBr): 2153 cm^{-1}; elemental analyses calcd for $C_{43}H_{27}N_2F_2Au\cdot H_2O$ (found): C 62.63 (62.64), H 3.54 (3.33), N 3.40 (3.19).

OLED Fabrication and Measurement. OLEDs were fabricated on patterned ITO-coated glass substrates with a sheet resistance of 30 Ω/□. The substrates were cleaned with Decon 90, rinsed with deionized water then dried in an oven, and finally treated in an ultraviolet−ozone chamber. A 70-nm thick α-naphthylphenylbiphenyl diamine (NPB) was used as the hole-transporting layer (HTL), and a 5-nm thick 4,4′-*N*,*N*′-dicarbazole-biphenyl (CBP) was used as the carrier confinement layer. A 30-nm thick emissive layer (EML) consisting of 1, 2, 4, and 6% complex **1** was doped into the CBP layer via thermal co-deposition. A 30-nm thick layer of aluminum(III) bis(2-methyl-8-quinolinato)-4-phenylphenolate (BAlq) and LiF/Al were used as the electron-transporting layer and metal cathode, respectively. All films were sequentially deposited at a rate of 0.1−0.2 nm/s without vacuum break. A shadow mask was used to define the cathode and to make four 0.1 cm^2 devices on each substrate. Current density−voltage−luminance (J−V−L) characteristics and electroluminescence (EL) spectra were measured simultaneously with a programmable Keithley model 237 power source and a Photoresearch PR650 spectrometer.

Acknowledgment. V.W.-W.Y. acknowledges support from The University of Hong Kong under the Distinguished Research Achievement Award Scheme and the URC Strategic Research Theme on Molecular Materials. This work has been supported by the University Grants Committee Areas of Excellence Scheme (AoE/P-03/08) and the UGC Special Equipment Grant (SEG-_HKU07). V.K.-M.A. and D.P.-K.T. acknowledge the receipt of postgraduate studentships from The University of Hong Kong.

Supporting Information Available: Crystallographic data for the structure of **1**. This material is available free of charge via the Internet at http://pubs.acs.org.

JA106579D

(28) *SAINT+, SAX area detector integration program*, Version 7.34A; Bruker AXS, Inc.: Madison, WI.
(29) Sheldrick, G. M. *SADABS,Empirical Absorption Correction Program.*; University of Göttingen, Göttingen, Germany, 2004.
(30) Sheldrick, G. M. *SHELXS 97, Programs for Crystal Structure Analysis*, Release 97-2; University of Göttingen: Göttingen, Germany, 1997.